Available online at www.sciencedirect.com

ScienceDirect

Natural Gas Industry B 9 (2022) 365−375

www.keaipublishing.com/en/journals/natural-gas-industry-b/

Research Article

Pore characterization of unconventional reservoirs

Shuheng Du[a,b]

[a] State Key Laboratory of Nonlinear Mechanics, Institute of Mechanics, Chinese Academy of Sciences, Beijing 100190, China

[b] School of Engineering Science, University of Chinese Academy of Sciences, Beijing 100049, China

Received 28 March 2022; revised 18 May 2022; accepted 21 July 2022

Available online 21 August 2022

Abstract

This study proposes an image-based idea for analyzing the complex geometric characteristics of reservoir spaces using various change curves of the pore geometric attributes to subdivide and evaluate tight reservoir rocks from micron to centimeter thicknesses. Using advanced imaging and image-processing technologies, in this study, we transform information from reservoir images into a vertical stratigraphy via an imaging-based method. The new parameter system incorporates three categories of parameters, size (S), morphology (M), and direction (D), to quantitatively and comprehensively characterize the pores of unconventional reservoir rocks. Given these three categories of the parameters, the curve at a certain depth value can be used to clearly identify obvious interfaces, which constitute high tip values. These interfaces may indicate that the hydrodynamic conditions, stress conditions of the reservoir, temperature and pressure, or other physical or chemical conditions changed significantly at these points, allowing the sedimentary compaction process to be well documented at the microscale level. This indicates that, from a micro-level perspective, we can find micro-evidence of the hydrodynamic conditions at the time of formation. Such information can help strengthen our understanding of the geological formation processes of unconventional hydrocarbon reservoirs.

Keywords: Pore; Characterization; Unconventional reservoir; Image processing

1. Introduction

Nowadays, large amounts of crude oil and natural gas are beginning to be extracted from unconventional reservoirs such as tight sandstone, shale, volcanic rock, oil shale, and oil sand. Unconventional hydrocarbon resources have gradually become a main focus of energy exploration and development. Consequently, a series of geological and geotechnical scientific problems need to be explored [1−6]. Pores are where fluids exist and flow in these unconventional reservoirs. Therefore, a comprehensive characterization of the pore properties is of great significance when quantitatively exploring the distribution and flow characteristics of fluids during the sedimentation process [7−15].

Geologists usually record and explore sedimentary, compaction, and diagenesis processes from a macroscopic view via the size and arrangement of rock particles on geologic outcrops [16−19]. From a microscopic view, the formation of pores is closely related to the processes of rock particle deposition, compaction, diagenesis, and other similar developments [20−22]. Therefore, the degree of pore evolution in a certain direction can reflect the microscopic deposition, compaction, and diagenetic records to a large extent. Arns et al. used the Minkowski function and the K-means clustering method to specify the fine delamination and characterization of rocks. They obtained a one-dimensional log of the morphological (Minkowski) functionals over a sliding window as a basis for their multivariate classification. Using sandstone as an example, they divided its particles into three categories: fine, transitional, and coarse [23−29].

Rock slicing is the most intuitive and effective way to study the development of rock minerals and pores and has been widely used in energy research. In recent years, computed tomography, field emission scanning electron microscopy (FE-

E-mail address: dushuheng@imech.ac.cn (Shuheng Du).

Peer review under responsibility of Sichuan Petroleum Administration.

https://doi.org/10.1016/j.ngib.2022.07.006

SEM), focused ion beam scanning electron microscopy, and other digital core technologies have gradually been developed and have contributed to a series of important achievements in research concerning unconventional hydrocarbon reservoirs [30−37]. However, an inspection of former studies indicates that the information contained in thin rock slices has not been fully exploited. Geological information, such as the characteristics of the pore development and the direction of the mineral arrangement, has not been linked with the actual formation direction. Therefore, the information obtained cannot, at present, completely reflect the characteristics of the pore evolution over a small depth range (e.g., the micron grade). Consequently, this means that the available geological information cannot fully reflect the true characteristics of the sedimentation, compaction, and diagenesis of a deposit [38−47].

Geometric description and image-processing techniques provide a powerful tool for pore characterization. Via the construction and integration of mathematical data, the corresponding mathematical parameters can be given a geological significance, providing a deeper understanding of geological processes. According to current studies, it is believed that the level of pore characterization of unconventional reservoirs is moving from “fine quantification” to “precise quantification” [48−56].

While studies on pore characterization have gradually become more comprehensive, there are still abundant opportunities for additional research. For example, at present, most descriptions of pores focus on parameters such as the equivalent radius, tortuosity, and shape factor but discount other parameters. Therefore, new criteria need to be integrated into the parameter system for pore characterization such that descriptions of pore evolution features become more specific, allowing for more geological information to be identified [57−60].

This paper presents a new experimental idea for how to record the evolution process at microscale depths to study the effects of deposition, compaction, and diagenesis on pore development.

2. Methodology

The proposed technical process is shown in Fig. 1. Accordingly, the sample core was processed following the technological procedure outlined in Fig. 1.

Next, the reservoir core was sliced into thin sections and characterized via FE-SEM. Many pore types with different origins can be identified in the thin sections, including intergranular, corrosion, and intergranular (clay mineral accumulation) pores, as well as very tiny nanopores [61−64]. When the samples are processed according to the method outlined in Fig. 1, the order of the pore development can be observed. This ability to observe the order of the pore development provides a foundation to further study the pore changes along the formation direction.

The first panel in Fig. 1 can be used as an example to explore the variation in the intergranular pores along the direction of formation. The curves of all the pore parameters along the vertical direction (the sedimentary direction) were constructed to characterize the pore evolution characterization of a tight oil sandstone reservoir at microscale depths.

The original depth range of the reservoir in the FE-SEM image may be up to nearly 2800 μm; therefore, only the parts of the curves with a depth range of 150 μm, rather than the complete curves, are included to illustrate this method.

To study pore evolution at microscale depths in the vertical direction, all pore parameters are ranked according to the y-coordinate value of their centroid. Then, the average value of pores with the same y-coordinate are calculated to represent the average level of each parameter at a given y-coordinate value.

The curves of each pore parameter are built along the vertical direction (the sedimentary direction), and the geological significance of these curves is then investigated. The pore parameters introduced here are divided into three categories: size (S), morphology (M), and direction (D).

To comprehensively and precisely characterize the pore evolution, the parameters in the three categories are listed in Tables 1−3.

As can be seen in Table 1, for the size, five parameters need to be calculated: area (A), perimeter (P), radius (R_a), major (M_a), minor (M_i), Feret (F), and MinFeret (M_f). Note that the above three types of parameters can all be calculated and processed using ImageJ, a public domain software for processing and analyzing scientific images [40,60].

The area parameter indicates the actual size of the pore; the larger the area, the better the reservoir properties.

The perimeter parameter denotes the complexity of the pore boundary, where a higher perimeter value indicates a more complex seepage path.

The radius parameter is similar in meaning to the area parameter but reflects the equivalent size of the pore more directly. A larger radius implies better reservoir properties.

The major and minor parameters express the equivalent size of the pore in the two main directions after best ellipse fitting. Under the minor condition, a larger major parameter indicates a narrower pore and a longer streamline. Conversely, under the major condition, a larger minor parameter indicates a flatter pore and a shorter streamline.

The Feret and MinFeret parameters are similar to the major and minor parameters but indicate the actual length and width of the pore, respectively. Under the MinFeret condition, a larger Feret value indicates a narrower pore and a longer streamline. However, under the Feret condition, a larger MinFeret value indicates a flatter pore and a shorter streamline.

As can be seen in Table 2, we defined four parameters to characterize the pore morphology: aspect ratio (AR), roundness (R_n), solidity (S_o), and circularity (C)[40,60].

The aspect ratio indicates the ellipticity of a pore; a high aspect ratio corresponds to a narrow pore and a long streamline.

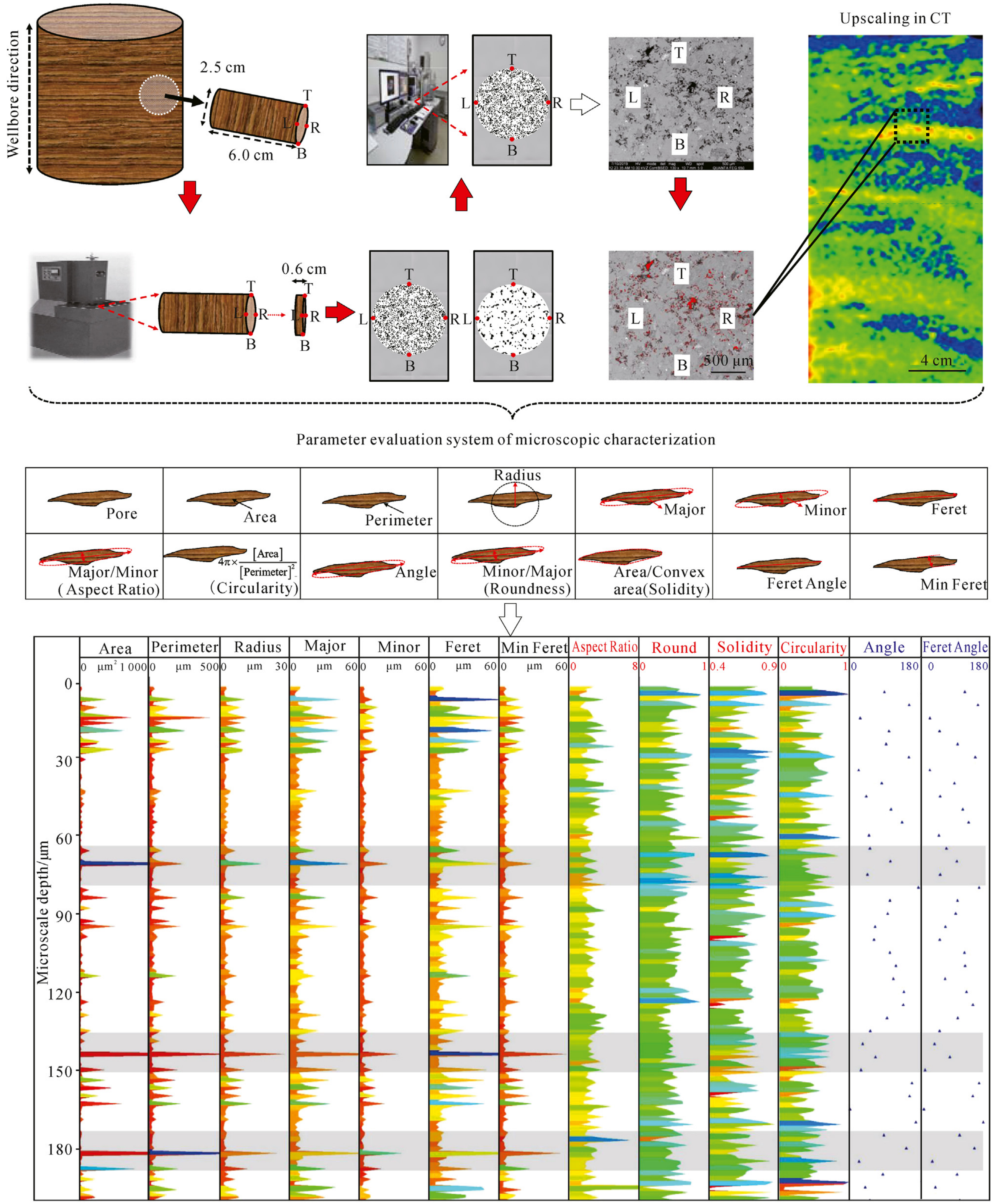

Fig. 1. Technical process for the construction of the various change curves of the pore geometric attributes. (Note that the computed tomography (CT) image does not show an actual sample from this study but is only used here to illustrate the experimental process.)

Table 1
Size parameters concerning the pore evolution in an unconventional hydrocarbon reservoir over a microscale depth range.

Parameter type	Parameter	Graphic explanation	Description
Size	A(Area)/μm^2	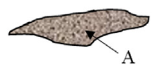	Area of pore
	P(Perimeter)/μm		Perimeter of pore
	R_a(Radius)/μm	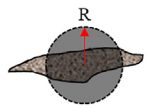	Equivalent radius of pore
	M_a(Major)/μm	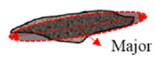	The primary axis of the best fitting ellipse.
	M_i(Minor)/μm	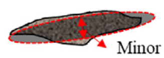	The secondary axis of the best fitting ellipse
	F(Feret)/μm	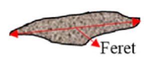	The longest distance between any two points along pore boundary
	M_f(MinFeret)/μm		The shortest distance between any two points along pore boundary

Table 2
Morphologic parameters concerning the pore evolution in an unconventional hydrocarbon reservoir over a microscale depth range.

Parameter type	Parameter of pore	Graphic explanation	Description
Morphology	AR(Aspect Ratio)		The aspect ratio of the particle's fitted ellipse
	R_n(Roundness)	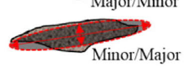	The inverse of Aspect Ratio
	S_o(Solidity)	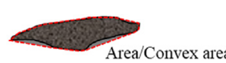	Concavity of pore
	C(Circularity)	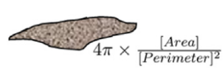	Circularity of pore

Table 3
Direction parameters concerning the pore evolution of an unconventional hydrocarbon reservoir over a microscale depth range.

Parameter type	Parameter of pore	Graphic explanation	Description
Direction	A_n(Angle)/°	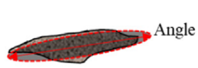	The angle between the primary axis and a line parallel to the X-axis
	FA(Feret Angle)/°		The angle of the between the Feret and a line parallel to the X-axis

Roundness is similar to the aspect ratio; however, a greater roundness indicates a flatter pore and a shorter streamline.

The solidity expresses the compaction degree of a pore. A larger solidity value indicates a lower compaction degree of the pore.

The circularity signifies the actual circular degree of a pore. A higher circularity value indicates a more circular pore and a shorter streamline.

As can be seen in Table 3, with respect to the direction, there are two parameters used Angle and Feret Angle [40,60].

The Angle parameter designates the equivalent extension direction of the pore after fitting, while the Feret Angle parameter measures the actual extension direction of the pore. The values of these two parameters reflect the dominant flow direction during the deposition process. Meanwhile, for pores in the same field of view, after obtaining their extension angles, we can evaluate the consistency of the pore angles by calculating the standard deviation of all of the angles. A smaller standard deviation indicates a higher consistency of the pore extension angle.

For example, in Fig. 1, the precise pore evolution can be clearly seen in the three categories of size (S), morphology (M), and direction (D). For the size and morphology parameters, the curve at a certain depth value can clearly indicate obvious interfaces, i.e., a high tip value. These interfaces may indicate a significant change in the hydrodynamic conditions, the stress conditions of the reservoir, the temperature and pressure, or other physical or chemical conditions, allowing the sedimentary compaction process to be well documented at the microscale level. For the direction parameters, there are corresponding turning points in the curves at certain depths. These turning points indicate transformations of the paleo flow direction during the deposition and compaction processes; this constitutes the most direct evidence available for the determination of the paleo flow direction at the microscale. This determination is therefore of great theoretical and practical significance.

3. Results and discussion

We selected samples from shale oil reservoirs in the Lucaogou Formation in Jimusar Sag, Junggar Basin, western Xinjiang, China, and subjected them to fine electron microscopy imaging (Figs. 2 and 3). Then, the variation laws of the pore geometry attributes were studied from the following three different perspectives.

3.1. Pores at large scales

The shale oil reservoir samples were sliced and ground in eight directions; then, fine electron microscopy imaging of the rock slices in the eight directions was performed. Note that the core used in this study is a sample with a diameter of 2.5 cm and a length of 8 cm. The core was cut every 22.5° to obtain slices in eight directions. This method is proposed in this study to characterize the microscopic anisotropy and heterogeneity of the samples [61].

We can qualitatively describe the heterogeneity and anisotropy of the reservoir via the eight-direction electron microscopy imaging. However, this only provides a qualitative characterization. Using the proposed method, we are able to establish curves of the various geometric attributes of the reservoir in different directions, as shown in Fig. 4.

From Fig. 4-a, we can see that at a depth of approximately 1000 μm, the morphological parameters of the pore form a significant turning point even though the size parameters of the pore are nearly unchanged. Specifically, in the reservoir area (at a depth higher than 1000 μm), the roundness is higher, the shape factor is higher, and the porosity is lower. In the area with a depth of less than 1000 μm, the roundness and shape factors decrease and the porosity increases. As far as the directivity parameters are concerned, the direction of the pores changes greatly with respect to that at 1000 μm. This indicates that 1000 μm is an important turning point. Both the main direction of the hydrodynamic force and the pore formation ability changed significantly at this point. This shows that, from a micro-level perspective, we can indeed find micro-evidence of the hydrodynamic conditions present during pore formation.

3.2. Pores related to the key mineral

In the shale oil reservoirs in the study area, feldspar is abundantly developed, resulting in a large number of primary and secondary pores related to feldspar, primarily intragranular corrosion pores caused by feldspar self-dissolution. This type of pore is one of the most important pore types in shale oil reservoirs and plays an extremely important role in oil reservoir and seepage processes.

Accordingly, the development of feldspar pores deserves attention. As before, we sliced and ground the shale oil reservoir samples in eight directions and performed fine electron microscopy imaging for the feldspar in the eight directions (Fig. 3). The pore anisotropy of the large horizon is very similar to that of the feldspar.

From Fig. 5-a, we can see that at a depth of approximately 100 μm, the morphological parameters of the feldspar pores form a significant turning point; however, the size parameters of the feldspar pores do not change significantly. Specifically, in the reservoir area with the depth of higher than 100 μm, the roundness is higher, the shape factor is higher, and the porosity is lower. The roundness and shape factor decrease and the pore concavity increases in the area with the depth of less than 100 μm (Fig. 5-a).

Meanwhile, the feldspar pores change greatly for lengths greater than approximately 150 μm. This indicates that the main direction of the hydrodynamic force and the secondary pore formation ability changed significantly at approximately 150 μm. Therefore, it is reasonable to conclude that the heterogeneity of the pore development requires additional attention when studying the mineral grade because there is a large amount of micro-evidence contained within the pores of minerals (Fig. 5-a and 5-b).

The above results show that the reservoir heterogeneity is very obvious in the microscopy and that research on this aspect of reservoirs cannot be ignored.

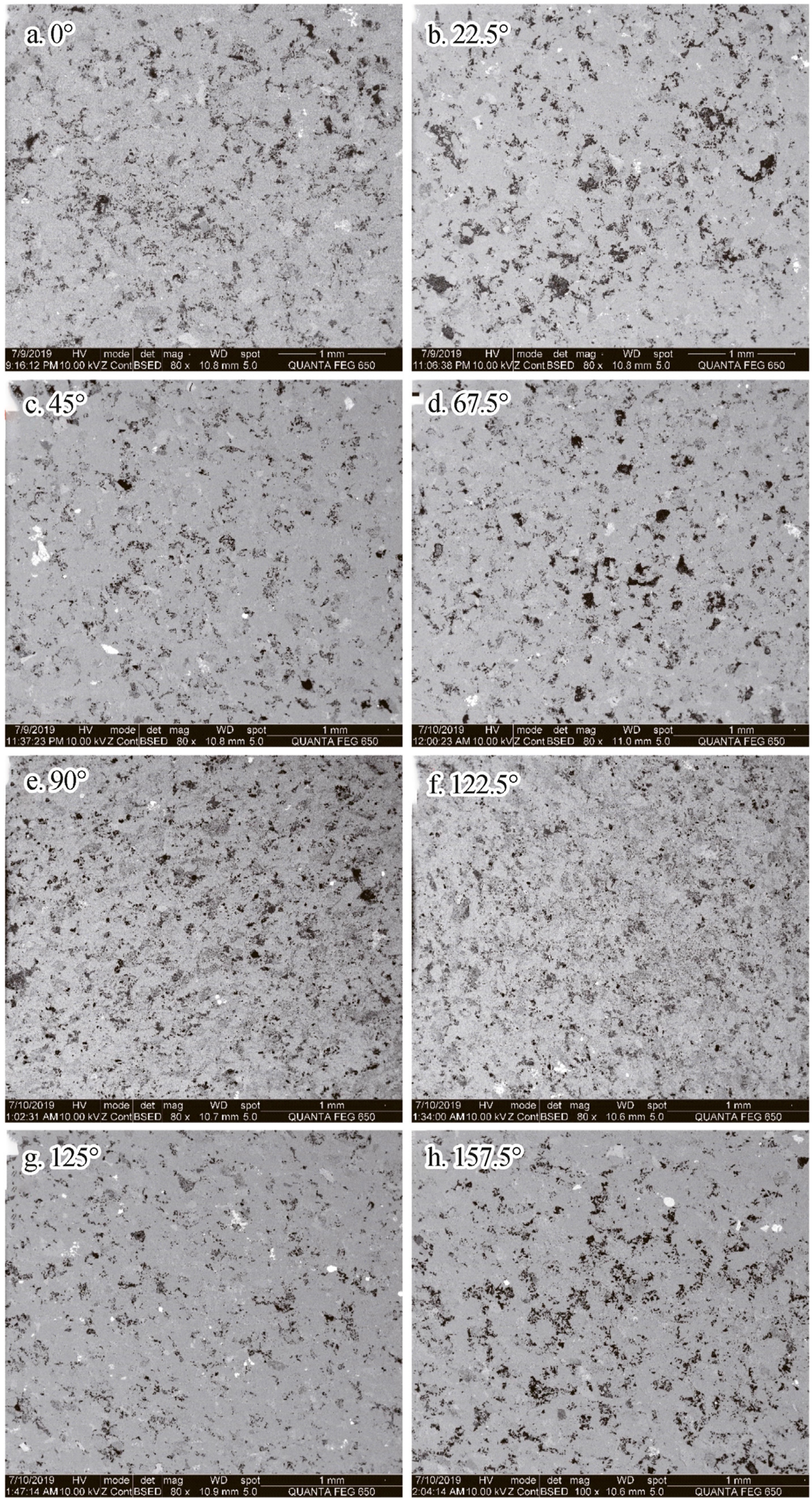

Fig. 2. Electron microscopy imaging of the pore development in a shale oil reservoir in the large visual field in eight different directions: (a) 0°; (b) 22.5°; (c) 45°; (d) 67.5°; (e) 90°; (f) 122.5°; (g) 125°; and (h) 157.5°.

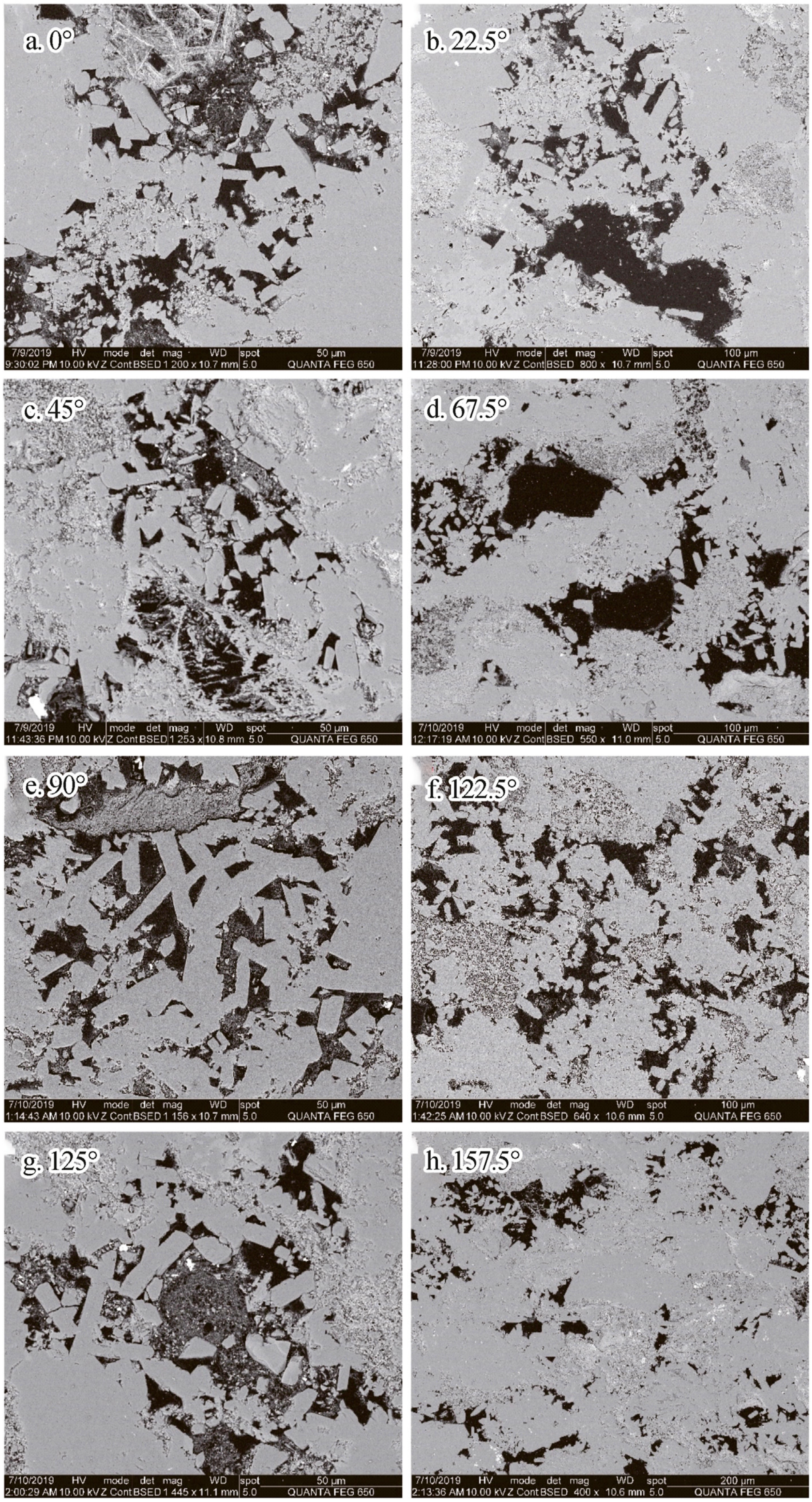

Fig. 3. Electron microscopy imaging of the pore development of feldspar in a shale oil reservoir in eight different directions: (a) 0°; (b) 22.5°; (c) 45°; (d) 67.5°; (e) 90°; (f) 122.5°; (g) 125°; and (h) 157.5°.

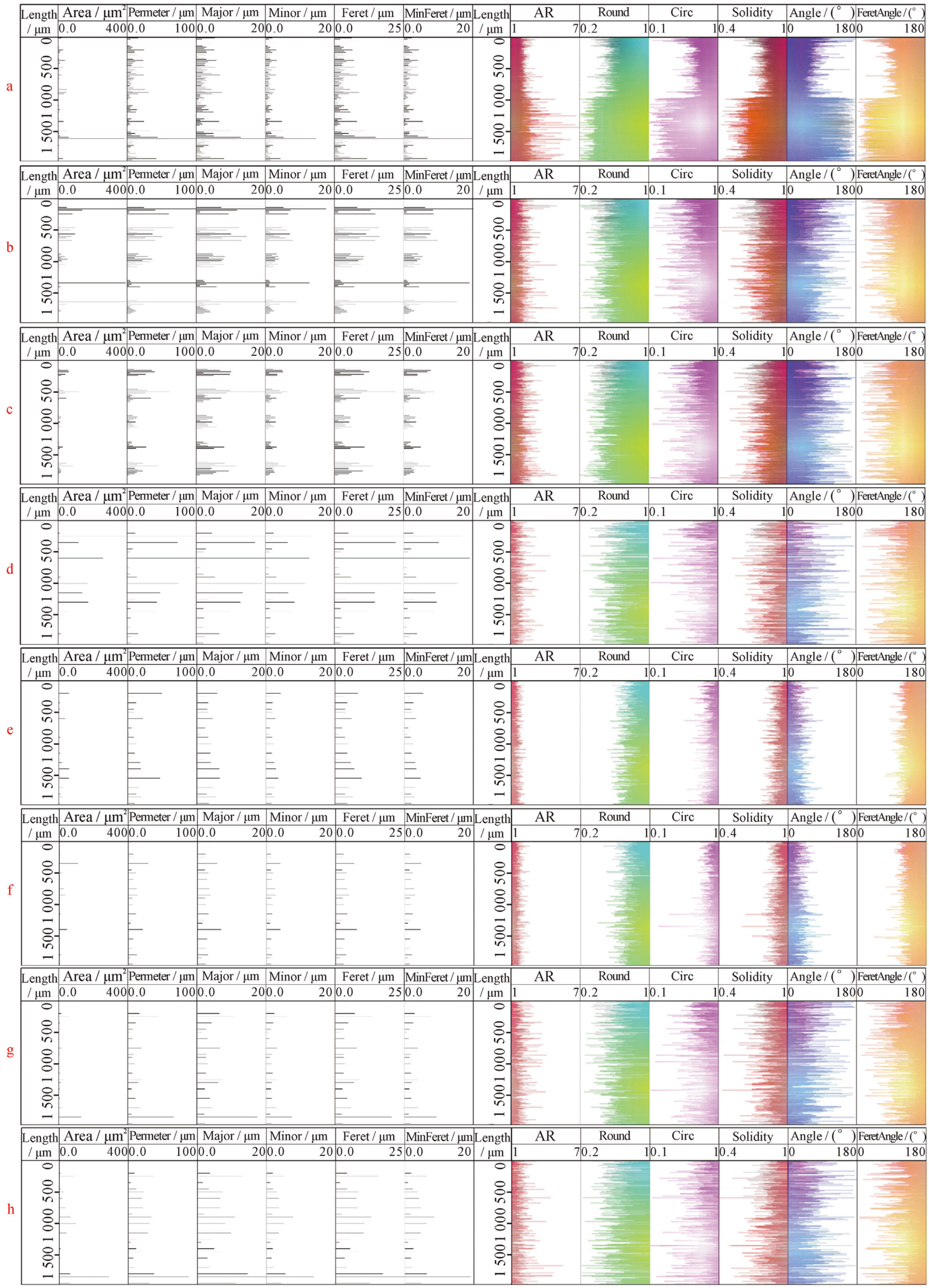

Fig. 4. Construction of the various change curves of the pore geometric attributes. (pores at large scales): (a) 0°; (b) 22.5°; (c) 45°; (d) 67.5°; (e) 90°; (f) 122.5°; (g) 125°; and (h) 157.5°.

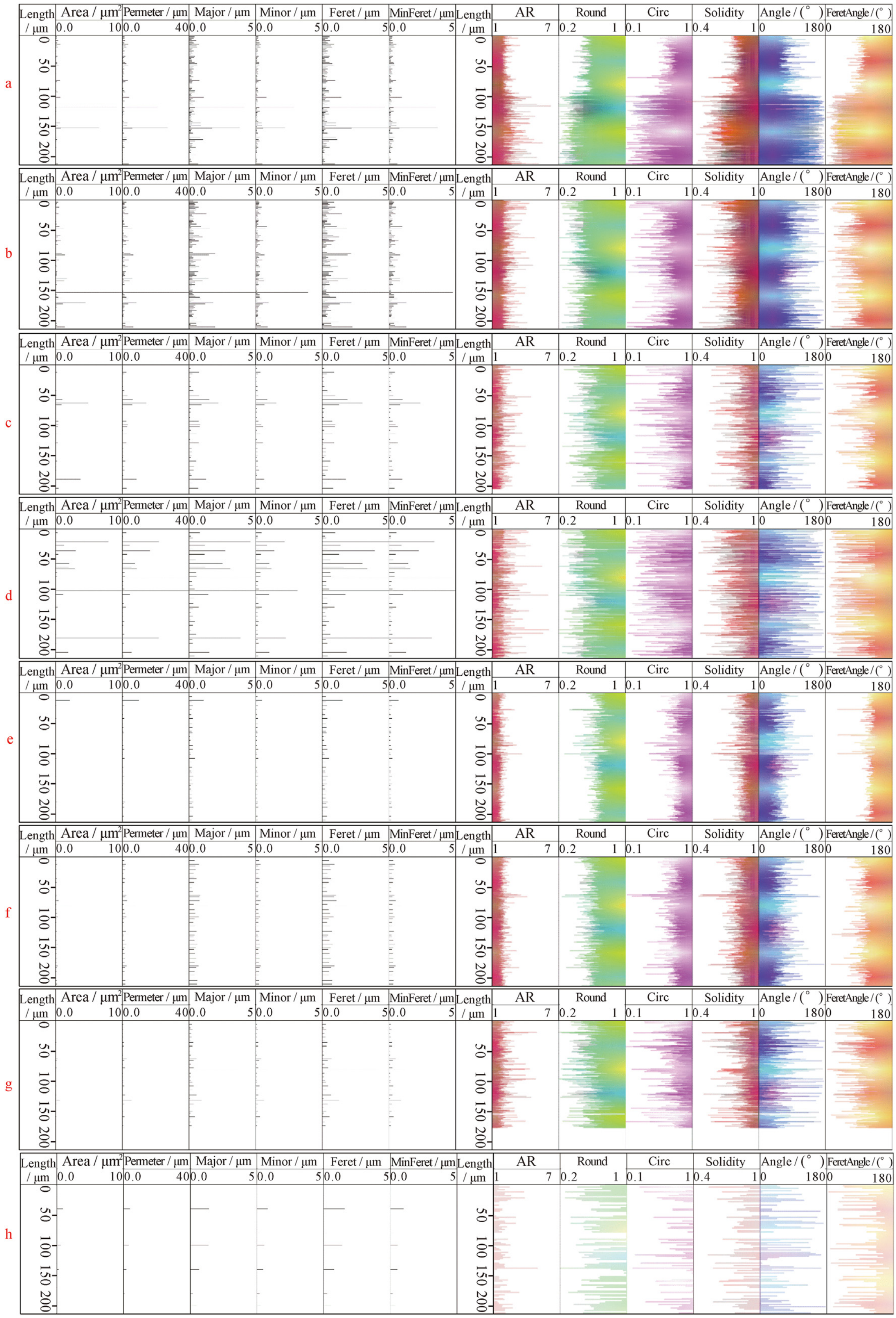

Fig. 5. Construction of the various change curves of the pore geometric attributes (pores related to the feldspar): (a) 0°; (b) 22.5°; (c) 45°; (d) 67.5°; (e) 90°; (f) 122.5°; (g) 125°; and (h) 157.5°.

4. Conclusions

The precise description of pores in unconventional hydrocarbon reservoirs is currently an important and much studied issue. At the same time, applying the precise identification of pore information to analyses of actual geological processes is an urgent problem. An effective method to construct the various change curves of the pore geometric attributes to subdivide and evaluate unconventional reservoir rocks in micron to centimeter thicknesses will benefit the exploration of reservoirs.

Using an innovative method incorporating advanced imaging and image-processing technologies, this paper transfers information from reservoir imaging into a vertical stratigraphy by establishing three parameter categories, size (S), morphology (M), and direction (D), that characterize the pore evolution of unconventional hydrocarbon reservoirs at microscale depths. In this new experimental approach, the disciplines of mathematics, computer science, and geology are combined to better analyze specific scientific problems.

Identifying a typical interface or turning point of a curve accurately allows the characteristics of the geological conditions in the sedimentary process to be analyzed and provides important theoretical guidance for the determination of geological factors such as the direction of the paleo flow, the hydrodynamic conditions, the stress state of the reservoir, and the temperature and pressure.

Conflicts of interest

The authors declare that they have no known competing financial interests or personal relationships that could have appeared to influence the work reported in this paper.

Acknowledgements

This work was supported by National Natural Science Foundation of China (NSFC, Grant No.41902132,12032019).

References

[1] Chen FX, Zhang HX & Zhuang Q. The quasi-static response of granular materials to a concentrated loading. Chin J Appl Mech 2015;32(2):244−50.
[2] Gao ZY, Fan YP, Hu QH, Jiang ZX, Huang ZL, Wang QY, et al. Differential development characteristics of organic matter pores and their impact on reservoir space of Longmaxi Formation shale from the South Sichuan Basin. Pet Sci Bull 2020;5(1):1−16.
[3] Huang XZ, Chen HN, Liu Y, Xiao JC & Wang QY. Study on and comparative analysis of concrete fracture properties using ESPI and DIC technologies. Chin J Appl Mech 2018;35(5):1131−8.
[4] Larionov KB, Mishakov IV, Slyusarskiy KV & Vedyagin AA. Intensification of bituminous coal and lignite oxidation by copper-based activating additives. Int J Coal Sci Technol 2021;8(1):141−53.
[5] Lei GY, Han JC, Dang FN, Li J, Li JB & Chen C. Comparative analysis of microscopic concrete numerical model. Chin J Appl Mech 2017;34(2):318−23.
[6] Li AF, Ren XX, Wang GJ, Wang YZ & Jiang KL. Characterization of pore structure of low permeability reservoirs using a nuclear magnetic resonance method. J China Univ Pet (Ed Nat Sci) 2015;39(6):92−8.
[7] Li J, Li XF, Chen ZX, Wang XZ, Wu KL, Sun Z, et al. Permeability model for gas transport though shale nanopores with irreducible water saturation. Pet Sci Bull 2018;3(2):167−82.
[8] Li JJ, Su H, Jiang HQ, Yu FW, Liang TB, Zhao YY, et al. Application of microfluidic models in the oil and gas field development. Pet Sci Bull 2018;3(3):284−301.
[9] Li RL, Zhou GQ, Yan K, Chen J, Chen DQ, Cai SY, et al. Preparation and characterization of a specialized lunar regolith simulant for use in lunar low gravity simulation. Int J Min Sci Technol 2022;32(1):1−15.
[10] Liu G & Chen YJ. Analysis on velocity of the water droplet in oil based on PIV. Chin J Appl Mech 2017;34(5):912−8.
[11] Luo XP, Zhang YB, Zhou HP, He KZ, Zhang BY, Zhang DM, et al. Pore structure characterization and seepage analysis of ionic rare earth orebodies based on computed tomography images. Int J Min Sci Technol 2022;32(2):411−21.
[12] Shi GX, Kou G, Du SH, Wei Y, Zhou W, Zhou B, et al. What role would the pores related to brittle minerals play in the process of oil migration and oil & water two-phase imbibition? Energy Rep 2020;6:1213−23.
[13] Wang ZY, Li HX, Lan XM, Wang K, Yang Y & Lisitsa V. Formation damage mechanism of a sandstone reservoir based on micro-computed tomography. Adv Geo-Energy Res 2021;5(1):25−38.
[14] Xi SJ, Zuo YJ, Sun WJB, Wu ZH & Liu H. Research on failure process of concrete with defects based on digital image processing. Chin J Appl Mech 2020;37(1):448−54.
[15] Xue DJ, Zhang ZP, Chen C, Zhou J, Lu L, Sun XT, et al. Spatial correlation-based characterization of acoustic emission signal-cloud in a granite sample by a cube clustering approach. Int J Min Sci Technol 2021;31(4):535−51.
[16] Yan KL, Guo XY & Xia ZY. The experimental study on the characteristics of turbulent boundarylayer based on the PIV technology of non-uniform interrogation window. Chin J Appl Mech 2021;38(4):1293−300.
[17] Zhang YB, Zhang BY, Yang SQ, Zhong ZG, Zhou HP & Luo XP. Research status of sandy conglomerates reservoir. J Yangtze Univ (Nat Sci Ed) 2011;8(3):63−6.
[18] Zhang YB, Zhang BY, Yang SQ, Zhong ZG, Zhou HP & Luo XP. Enhancing the leaching effect of an ion-absorbed rare earth ore by ameliorating the seepage effect with sodium dodecyl sulfate surfactant. Int J Min Sci Technol 2021;31(6):995−1002.
[19] Zhang WD, Fan JL, Chen L & Fan YY. Study on the application of two-dimensional digital image correlation method in quasi-static tension test. Chin J Appl Mech 2018;35(5):1058−64.
[20] Dong H. Micro-CT imaging and pore network extraction. London: Imperial College; 2007 (Doctoral dissertation, PhD dissertation).
[21] Zhao JL, Sun MD, Pan ZJ, Liu B, Ostadhassan M & Hu Q. Effects of pore connectivity and water saturation on matrix permeability of deep gas shale. Adv Geo-Energy Res 2022;6(1):54−68.
[22] Zheng YC, Han X, Zeng J, Zhou CL, Zhou L & Chen WH. Practice of high-intensity volume fracturing in the Shaximiao Formation tight sandstone gas reservoirs of the Qiulin Block, central Sichuan Basin. Nat Gas Ind B 2021;8(4):367−75.
[23] Arns CH, Mecke J, Mecke K & Stoyan D. Second-order analysis by variograms for curvature measures of two-phase structures. Eur Phys J B 2005;47(3):397−409.
[24] Arns CH. The influence of morphology on physical properties of reservoir rocks. 2002 (Doctoral dissertation, University of New South Wales).
[25] Jin ZJ, Zhang JC & Tang X. Unconventional natural gas accumulation system. Nat Gas Ind B 2022;9(1):9−19.
[26] Chen SB, Zhang C, Li XY, Zhang YK & Wang XQ. Simulation of methane adsorption in diverse organic pores in shale reservoirs with multi-period geological evolution. Int J Coal Sci Technol 2021;8(5):844−55.
[27] Chen X, Zheng LG, Jiang YL & Jiang CL. Transformation of minerals at the boundary of magma-coal contact zone: case study from Wolonghu Coal Mine, Huaibei Coalfield, China. Int J Coal Sci Technol 2021;8(1):168−75.
[28] Hou WT, Wang HP, Yuan L, Wang W, Xue Y & Ma ZW. Experimental research into the effect of gas pressure, particle size and nozzle area on initial gas-release energy during gas desorption. Int J Min Sci Technol 2021;31(2):253−63.

[29] Jiang YD, Mo WF, Cao TY, Shi YX & Cai NS. Fabrication and performance of atmospheric plasma sprayed solid oxide fuel cells with liquid antimony anodes. Int J Coal Sci Technol 2021;8(3):360−7.
[30] Li JR, Yang Z, Wu ST & Pan SQ. Key issues and development direction of petroleum geology research on source rock strata in China. Adv Geo-Energy Res 2021;5(2):121−6.
[31] Liu A, Liu SM, Liu P & Wang K. Water sorption on coal: effects of oxygen-containing function groups and pore structure. Int J Coal Sci Technol 2021;8(5):983−1002.
[32] Ping A, Xia WC, Peng YL & Xie GY. Comparative filtration and dewatering behavior of vitrinite and inertinite of bituminous coal: experiment and simulation study. Int J Min Sci Technol 2021;31(2):233−40.
[33] Qin JH, Zheng J & Li L. An analytical solution to estimate the settlement of tailings or backfill slurry by considering the sedimentation and consolidation. Int J Min Sci Technol 2021;31(3):463−71.
[34] Wang G, Qin XJ, Han DY & Liu ZY. Study on seepage and deformation characteristics of coal microstructure by 3D reconstruction of CT images at high temperatures. Int J Min Sci Technol 2021;31(2):175−85.
[35] Zhong GF, Zhang D & Zhao LX. Current states of well-logging evaluation of deep-sea gas hydrate-bearing sediments by the international scientific ocean drilling (DSDP/ODP/IODP) programs. Nat Gas Ind B 2021;8(2):128−45.
[36] Du SH. Characteristics and the formation mechanism of the heterogeneous microfractures in the tight oil reservoir of Ordos Basin, China. J Petrol Sci Eng 2020;191, 107176.
[37] Huang X, Gao H & Du LB. Micro pore structure and water-flooding characteristics on tight sandstone reservoir. Journal of China University of Petroleum (Edition of Natural Science) 2020;44(1):80−8.
[38] Zhang L, Kang LX, Jing WL, Guo YH, Sun H, Yang YF, et al. Flow behavior analysis of oil-water two-phase flow in pore throat doublet model. J China Univ Pet (Ed Nat Sci) 2020;44(5):89−93.
[39] Liao GZ, Li YZ, Xiao LZ, Qin ZJ, Hu XY & Hu FL. Prediction of microscopic pore structure of tight reservoirs using convolutional neural network model. Pet Sci Bull 2020;5(1):26−38.
[40] Zeng YJ, Du SH, Zhang X, Zhang BP & Liu HL. The crucial geometric distinctions of microfractures as the indispensable transportation channels in hydrocarbon-rich shale reservoir. Energy Rep 2020;6: 2056−65.
[41] Zou GG, She JS, Peng SP, Yin QC, Liu HB & Che YY. Two-dimensional SEM image-based analysis of coal porosity and its pore structure. Int J Coal Sci Technol 2020;7(2):350−61.
[42] Cai LX, Xiao GL, Lu SF, Wang J & Wu ZQ. Spatial-temporal coupling between high-quality source rocks and reservoirs for tight sandstone oil and gas accumulations in the Songliao Basin, China. Int J Min Sci Technol 2019;29(3):387−97.
[43] Du SH, Shi GX, Yue XJ, Kou G, Zhou B & Shi YM. Imaging-based characterization of perthite in the upper triassic yanchang formation tight sandstone of the ordos basin, China. Acta Geol Sin English Ed 2019;93(2):373−85.
[44] Du SH, Zhao YP, Jin J, Kou G, Shi YM & Huang XF. Significance of the secondary pores in perthite for oil storage and flow in tight sandstone reservoir. Mar Petrol Geol 2019;110:178−88.
[45] Wang M, Huang K, Xie WD & Dai XG. Current research into the use of supercritical CO2 technology in shale gas exploitation. Int J Min Sci Technol 2019;29(5):739−44.
[46] Wang YC, Jiang HQ, Yu FW, Cheng BY, Xu F & Li JJ. Researches on the pore permeability prediction method of 3D digital cores based on machine learning. Pet Sci Bull 2019;4(4):354−63.
[47] Zhuravlev YN & Porokhnov AN. Computer simulation of coal organic mass structure and its sorption properties. Int J Coal Sci Technol 2019;6(3):438−44.
[48] Qu M, Hou JR, Li J, Tan T, Guo C & Shi YL. Research into characteristics of the oil-water interface during bottom water flooding in a fractured-vuggy reservoir by a 3-D visual model. Pet Sci Bull 2018;3(4):422−33.
[49] Du SH, Shi YM, Guan P & Zhang YG. New inspiration on effective development of tight reservoir in secondary exploitation by using rock mechanics method. Energy Explor Exploit 2016;34(1):3−18.
[50] Luo R, Zha M, He H, Gao CH, Qu JX, Hua ZF, et al. Characteristics of pore structures in paleogene shales in Nanpu Sag. J China Univ Pet (Ed Nat Sci) 2016;40(2):23−33.
[51] Sun P, Tang YJ, Zhang YS & Peng Y. The characteristics of biomarker compounds of source rocks in Linxi formation in Guandi section of Linxi county in the east of Inner Mongolia. J Yangtze Univ (Nat Sci Ed) 2016;13(32):1−6.
[52] Wan YZ & Zhang NN. Analysis on provenance in huagang formation of xihu depression in the East China Sea basin. J Yangtze Univ (Nat Sci Ed) 2016;13(35):24−7.
[53] Zhang Y, Wang QB, Wang FL, Lu H & Cui HZ. Characteristics and control factors of biodegradation of crude oil in LD16-A and LD16-B structures of Bohai Sea. J Yangtze Univ (Nat Sci Ed) 2016;13(29):13−7.
[54] Chen K, He WX & Wei J. Application of interwell tracer method in analysis of reservoir connectivity. J Yangtze Univ (Nat Sci Ed) 2015;12(8):70−3.
[55] Li JJ, Shi YL, Huang ZK, Wang WM, Cao Q & Lu SF. Pore characteristics of continental shale and its impact on storage of shale oil in northern Songliao Basin. J China Univ Pet (Ed Nat Sci) 2015;39(4):27−34.
[56] Sun KM, Xin LW & Zhang SC. Permeability variation law of porous media during heating process under effect of initial geostress. J China Univ Pet (Ed Nat Sci) 2015;39(3):138−42.
[57] Li D, Fei CG & Wang NN. Evaluation and analysis of field tests for polysurfactant. J Yangtze Univ (Nat Sci Ed) 2013;10(16):128−34.
[58] Dong WJ, Zhu YX & Wan MG. Identification and classification of sedimentary environment based on Fisher discriminant analysis. J Yangtze Univ (Nat Sci Ed) 2011;8(5):5−7.
[59] Pang QW, Wang ZQ, Qin Y & Fu H. Tracer analysis of hydrocarbon migration in Baijiahai arch-Fubei slope of Junggar basin. J Yangtze Univ (Nat Sci Ed) 2011;8(12):40−2.
[60] Website. https://imagej.nih.gov/ij/.
[61] Du SH, Pang S, Chai GS & Shi YM. Quantitative analysis on the microscopic anisotropy characteristics of pore and mineral in tight reservoir by "umbrella deconstruction" method. Earth Sci 2020;45(1):276−84.
[62] Du SH. Anisotropic rock poroelasticity evolution in ultra-low permeability sandstones under pore pressure, confining pressure, and temperature: experiments with biot's coefficient. Acta Geol Sin-English Ed 2021;95(3):937−45.
[63] Du SH, Shi YM & Guan P. Fluid filling rule in intra-granular pores of feldspar and fractal characteristics: a case study on yanchang formation tight sandstone reservoir in ordos basin. Earth Sci 2019;44(12):4252−63.
[64] Du SH & Shi YM. Rapid determination of complete distribution of pore and throat in tight oil sandstone of Triassic Yanchang Formation in Ordos Basin, China. Acta Geol Sin-English Ed 2020;94(3):822−30.